Analysis of Heat Transfer in Turbulent Channel Using Grooves

Mayank Bhola[1], Dr. Satyendra Singh[2]

[1]M. Tech Scholar, Department of Mechanical Engineering,
Bipin Tripathi Kumaon Institute of Technology, Dwarahat, Almora, Uttarakhand (India) 263653

[2]Associate Professor, Department of Mechanical Engineering,
Bipin Tripathi Kumaon Institute of Technology, Dwarahat, Almora, Uttarakhand (India) 263653

Abstract: ***This paper presents a numerical investigation of forced convection in a two-dimensional turbulent channel with periodic transverse grooves on the lower channel using CFD in ANSYS FLUENT. The lower wall is subjected to a uniform heat flux of 1000W/m^2 while the upper wall is insulated. To investigate effect of grooves on heat transfer and friction factor, computations based on a finite volume method, are carried out by utilizing Realizable k-ε turbulent model with non-equilibrium wall function. Parametric runs are made for Reynolds numbers ranging from 6000 to 18,000 with the groove-width to channel-height ratio (B/H) of 0.5 to 1.5 while the groove pitch ratio of 2 and the depth ratio of 0.5 are fixed throughout. It is found that the grooved channel provides a considerable increase in heat transfer of about 146% to 199% for different B/H values.***

Keywords: Turbulent channel, CFD, ANSYS FLUENT, Grooves, Realizable k-ε

1. Introduction

For well over few decades, efforts have been made for improving convective heat transfer in thermal system used in many engineering applications with a view of reducing weight size and cost of heat exchanger. The study of enhanced heat transfer has gained momentum during recent years, due to increased demands by industry for thermal system that are less expensive to build and operate than standard devices. Saving in material and energy use also provide motivation for the development of improved methods of enhancement. Recently heat exchanger of parallel plate with one plate having constant heat flux and other one insulated or adiabatic type have gained interest in agricultural industry for crop drying purposes, and for solar air heater, plates coated with absorber material are used due to increase in heat generation using solar energy.There are various ways to increase heat transfer in different equipment for different applications. Special surface geometries bring about the transport-enhancement by establishing a higher heat transfer coefficient. Protrusions can be mounted on the channel walls in order to generate longitudinal vortices which disrupt the growth of the boundary layer and also prevent fluid separation thereby enhance the heat transfer between the flowing fluid and the channel walls. Various heat transfer enhancement techniques are used such as fins, ribs, dimpled surfaces, and protruding surfaces that generate vortices in a heat exchanger. Enhancement techniques can be separated into two categories: passive and active. Passive methods require no direct application of external power. Instead, passive techniques employ special surface geometries or fluid additives which cause heat transfer enhancement. On the other hand, active schemes such as electromagnetic fields and surface vibration do require external power for operation. The majority of commercially interesting enhancement techniques are passive ones. Active techniques have attracted little commercial interest because of the cost involved, and the problems that are associated with vibration or acoustic noise. This work deals only with gas-side heat transfer enhancement using special surface geometries. Special surface geometries provide enhancement by establishing a higher heat transfer rate per unit base surface area. Clearly there are three basic ways of accomplishing this:

1. Increase the effective heat transfer surface area per unit volume without appreciably changing the heat transfer coefficient (h). Plane fin surfaces enhance heat transfer in this manner.
2. Increase h without appreciably change in area. This is accomplished by using a special geometrical shape, such as dimple, protruded or grooved mixing due to secondary flows and boundary-layer separation within the channel. Vortex generation also increases h without a significant area increase by creating longitudinal spiraling vortices exchange fluid between the wall and core regions of flow, resulting in increased heat transfer
3. Increase both h and A. Interrupted fins act this way. These surfaces increase the effective surface area, and enhance heat transfer through repeated growth and destruction of the boundary layers.

2. Literature Review

Lorenz, et. al. (1995) determined the distribution of heat transfer coefficient and pressure drop along the wall inside a ribbed channel for thermally developing and periodic turbulent flow experimentally, for measuring temperature distribution and Nusselt no. at ribbed wall they used infrared thermography. They reported an increase of 1.52 to 1.75 times in global Nusselt no. at the grooved wall as compared to a plane wall. Jaurker, et. al. (2005) investigated the heat transfer and friction factor characteristics of rib-grooved artificial roughness in solar air heater with relative roughness height 0.0181-0.0363, relative roughness pitch 4.5-10.0, and groove position to pitch ratio 0.3-0.7. They reported 2.7 times increase in Nusselt no. and 3.6 times rise in friction factor for the range of parameters investigated when compared to smooth tube, and also developed some statistical correlations for Nusselt no. as a function of rib-groove position, rib height, pitch and Reynolds number.

Eiamsa-ard and Promvonge (2008) numerically investigated turbulent forced convection in a 2-D channel with periodic transverse grooves utilizing four different turbulence models: the standard k−ε, the Renormalized Group (RNG) k−ε, the standard k−ω, and the shear stress transport (SST) k−ω turbulence models. With groove width to channel height ratio (B/H) of 0.5 to 1.75. They predicted that RNG and k−ε turbulence model provide better agreement than others and highest heat transfer is achieved for B/H 0.75, they also conclude that increase in recirculation flow helps in increasing the heat transfer Sahu and Gandhi (2014) numerically investigated the effect on heat transfer and flow field characteristics due to an inclined rib with a gap on solar air heater duct. They determined that Realizable k−ε turbulence model with standard wall function provides best result for these kind of problems to be solved numerically. However, the model fails to predict correctly the friction factor values for roughened plate. Kim and lee (2007) conducted a CFD simulation to optimize internal cooling passage using V-shaped ribs using shear stress transport (SST) model for several different Reynolds numbers. Rib pitch-to-rib height ratio, rib height-to-channel height ratio, and the attack angle of the rib. They concluded thatas design emphasis is shifted to reduction of friction loss, values of rib pitch-to-rib height ratio increases, but rib height-to-channel height ratio decreases. Luo et al (2006) performed a simulation on flow and forced-convection characteristics of turbulent flow through parallel plates with periodic transverse ribs using Reynolds stress model (RSM) for Reynolds number range of 20,000 to 94,000. The ribs were uniformly spaced with the pitch-to-height ratio of p/e = 4, a height-to-hydraulic-diameter ratio of e/D =0.25, and a width-to-height ratio of w/e = 2. A second-order upwind scheme was applied in the calculation and a very fine mesh density was arranged in the regions near the wall boundaries. The SIMPLE algorithm was adopted to handle the pressure–velocity coupling in the calculation. Local Nusselt number distribution along the heated bottom ribbed surface was investigated. They found that in the simulation of the turbulent forced convection in this two-dimensional channel with a ribbed surface, the standard k–e model had superiority over the Reynolds stress model. An anticlockwise vortex was found in the downstream region of a rib by using either of the two models; however, the length and relative strength of the vortex predicted by these two models were significantly different. Recirculating flow pattern was formed in the cavity between two adjacent ribs, while no reattachment of the mainstream flow was observed at the presented pitch-to-height ratio of p/e = 4. Chaube et al (2005) they carried out a computational analysis of heat transfer augmentation and flow characteristics due to artificial roughness for solar air heater in the form of ribs on a broad, heated wall of a rectangular duct for turbulent flow for Reynolds number range 3,000-20,000 using shear stress transport k-w turbulence model. They conducted the experiment for nine different types of ribs and compared on the basis of heat transfer enhancement. They concluded that the SST k- w model gives good results for the prediction of heat transfer and friction characteristics in high aspect ratio rib roughened rectangular duct. The model predicts well near the central high heat transfer area but it under predicts around ribs.

3. Mathematical Formulation

The system of interest is a horizontal plane channel with nine periodic grooves (eight ribs) along the lower channel wall as shown in Fig. 1. The channel height is set to H=40mm while the channel length, rib land (s) and groove width (B) were set to 47H, H and H, respectively. To ensure a fully developed flow, the first groove was located at the distance of 20H downstream of the entrance while the last groove was set to 10H upstream of the exit. The grooved channel having eight ribs with a test section length of L=680 mm (17H), 20 mm rib height (e=0.5H), 40 mm rib length (s=H) and 40 mm channel clear height (H) as depicted in Fig. 1. To examine an effect of the groove size on heat transfer and friction loss in the channel, the groove width ratio, (B/H), is varied to be B/H=0.5, 0.75, 1.0, 1.25, and 1.5, for each test run of calculations.

A uniform rectangular mesh with grid adoption for y+≈2.5 at an adjacent wall region is used to resolve the laminar sub-layer and is shown in Fig. 2. Number of elements are adopted as 144192. The mean inlet velocity between 1.19 and 3.58 m/s based on Reynolds number cited above, zero pressure gradients at the exit and no slip wall boundary conditions are taken for the present computation. In previous research, Chaube et al. [7] suggested that the calculation with 2- dimensional flow model yields the results closer to measurements as compared that with 3-dimensional flow. In this work, the 2D flow is therefore carried out for saving computer memory and computational time.

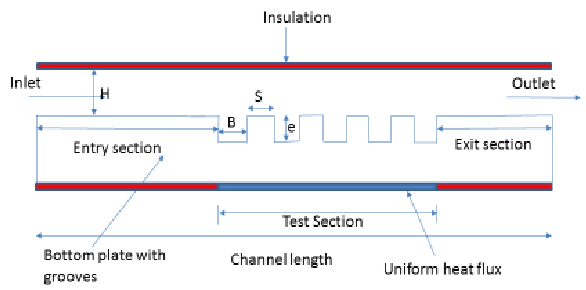

Figure 1: Schematic Diagram

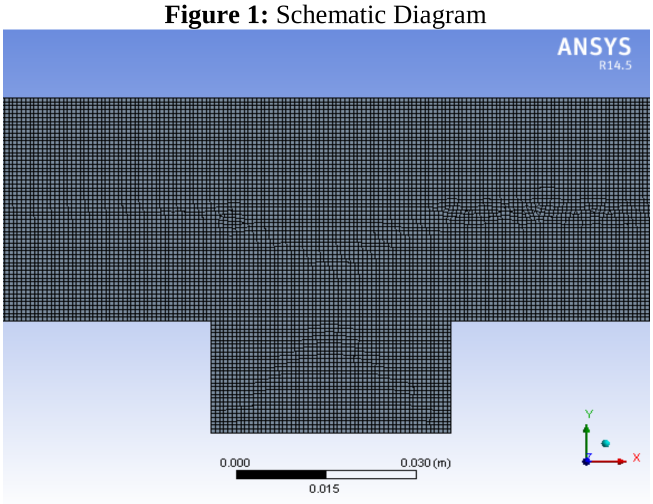

Figure 2: Meshing

4. Governing Equations

4.1 Continuity Equation

$$\frac{\partial\rho}{\partial t}+\frac{\partial}{\partial x}(\rho v_x)+\frac{\partial}{\partial y}(\rho v_y)+\frac{\partial}{\partial z}(\rho v_z)=0$$

4.2 Kappa-Epsilon Model

$$\rho[\bar{u}\frac{\partial k}{\partial x}+\bar{v}\frac{\partial k}{\partial r}]=\frac{\partial}{\partial x}[(\mu_l+\frac{\mu_t}{\sigma_k})\frac{\partial k}{\partial x}]+\frac{1}{r}\frac{\partial}{\partial r}[r(\mu_l+\frac{\mu_t}{\sigma_k})\frac{\partial k}{\partial r}]+\rho g-\rho\varepsilon$$

Where, G is the production term and is given by

$$G=\mu_t[2\{(\frac{\partial\bar{v}}{\partial r})^2+(\frac{\partial\bar{u}}{\partial x})^2+(\frac{\bar{v}}{r})^2\}+(\frac{\partial\bar{u}}{\partial r}+\frac{\partial\bar{v}}{\partial x})^2]$$

ε - Equation

$$\rho[\bar{u}\frac{\partial\varepsilon}{\partial x}+\bar{v}\frac{\partial\varepsilon}{\partial r}]=\frac{\partial}{\partial x}[(\mu_l+\frac{\mu_t}{\sigma_\varepsilon})\frac{\partial\varepsilon}{\partial x}]+\frac{1}{r}\frac{\partial}{\partial r}(r\mu_l+\frac{\mu_t}{\sigma_\varepsilon})\frac{\partial\varepsilon}{\partial r}]+$$

$$C_{S1}G\frac{\varepsilon}{k}-C_{S2}\frac{\varepsilon^2}{k}$$

Here C_{s1}, C_{s2}, σ_k and σ_ε are the empirical turbulent constant. The values are considered according to the Launder *et al.*, 1974. The values of Cμ, C_{s1}, C_{s2}, σ_k and σ_ε are 0.09, 1.44, 1.92, 1.0 and 1.3 respectively.

4.3 Energy Equation

The conservation form of energy equation written in terms of total energy is presented below.

$$\rho\frac{DE}{Dt}=-div(pu)+[\frac{\partial(u\tau_{xx})}{\partial x}+\frac{\partial(u\tau_{yx})}{\partial y}+\frac{\partial(u\tau_{zx})}{\partial z}+\frac{\partial(v\tau_{xy})}{\partial x}+\frac{\partial(v\tau_{yy})}{\partial y}+\frac{\partial(v\tau_{zy})}{\partial z}+\frac{\partial(w\tau_{xz})}{\partial x}+\frac{\partial(w\tau_{yz})}{\partial y}+\frac{\partial(w\tau_{zz})}{\partial z}+div(k\ grad\ T)+S_E]$$

4.4 Boundary Condition

A turbulent flow is considered. The quantities *U*, *k*, *ε* are obtained by using numerical calculations based on the *k-ε* model for high Reynolds Number. The boundary conditions are listed below:

1) At the inlet of the channel:

$u=U_{in}, v=0$

$k_{in}=0.005U_{in}^2$

$\varepsilon_{in}=0.1K_{in}^2$

K_{in} stands for the admission condition for turbulent kinetic energy and ε_{in} is the inlet condition for dissipation.

2) At the walls:

$u=v=0$

$k=\varepsilon=0$

3) At the exit:

$P=P_{atm}$

The Reynolds number based on circular diameter in case of circular tube and hydraulic diameter D_h in case of rectangular tube.

$$\mathrm{Re}=\frac{\rho.U_0.D_h}{\mu}$$

5. Solution Procedure

The time-independent incompressible Navier–Stokes equations and the turbulence model were discretized using the finite volume method. Second order upwind scheme was applied for convective and turbulent terms. To evaluate the pressure field, the pressure–velocity coupling algorithm SIMPLE (Semi Implicit Method for Pressure-Linked Equations) was selected. At the inlet, uniform velocity profile has been imposed. Impermeable boundary condition has been implemented over the channel wall while constant heat flux condition is applied to the lower wall of test section. The turbulence intensity was kept at 10% at the inlet. Two parameters of interest for present case are: (1) Nusselt Number (2) friction factor. The friction factor, f is computed by pressure drop, Δp across the length of test section, L, having the hydraulic diameter, D_h=2H as

$$f=\frac{\Delta p}{4(\frac{L}{D_h})\frac{\rho u^2}{2}}$$

The heat transfer is measured by Nusselt number which can be obtained by

$$Nu=\frac{h}{k/D_h}$$

6. Results

The results for smooth plate are calculated according to the correlation use by Lorenz et.al. [1], and the results for Nusselt number are compared from Eiamsa-ard and Promvonge [3]

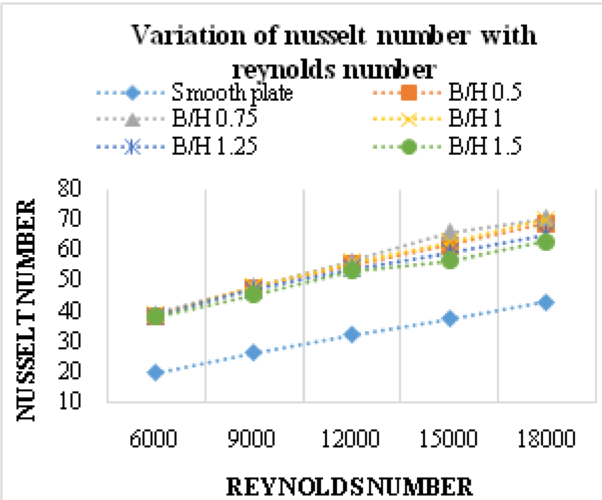

Figure 3: Variation of Nusselt number with Reynolds number

Fig. 3 shows the heat transfer results for air (T_i= 299 K) flow in the channel for five different groove width ratios (B/H= 0.5, 0.75, 1, 1.25, 1.5). In the figure, the Nusselt number are related as a function of Reynolds number. The results for smooth channel is also presented in the figure for comparison. Figure shows that the Nusselt number increases with increase in Reynolds number. In all cases, grooved channel flow gives higher value for Nusselt number than that for smooth channel flow due to induced turbulence. From figure it is also observed that for lower Reynolds number value of Nusselt number is nearly same for all B/H. The maximum Nusselt number is obtained for B/H= 0.75. The increase in Nusselt number values by using different ratios of B/H are about 146% to 199%.

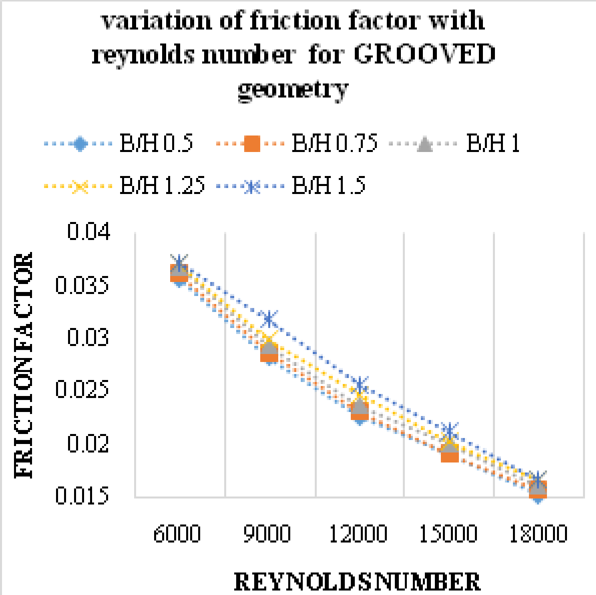

Figure 4: Variation of friction factor with Reynolds number

Fig.4 shows results for friction factor for different B/H ratios. It is observed that the friction factor decreases with increase in Reynolds number in all cases due to increase in pressure drop. Maximum friction factor is found for B/H 1.5. Contours of X-velocity at Reynolds number 12000 are also provided in Fig.5 showing the recirculation zone for different B/H ratios. It is observed that increase in ratio B/H also increases recirculation zone.

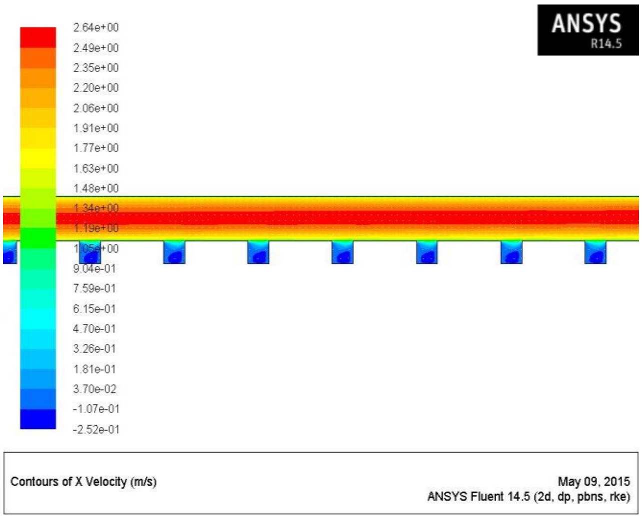

A

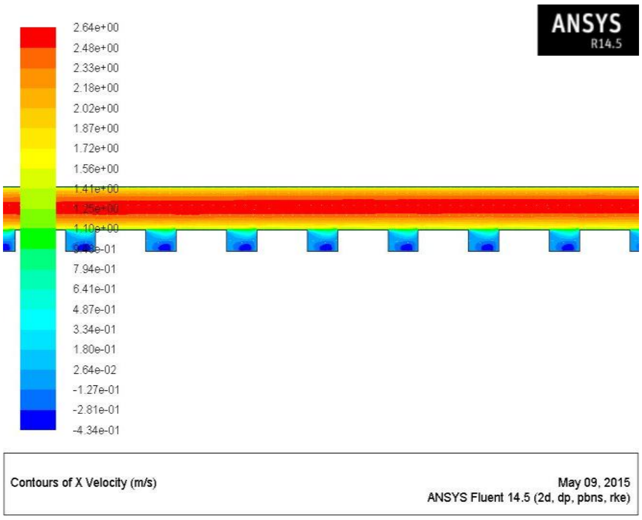

B

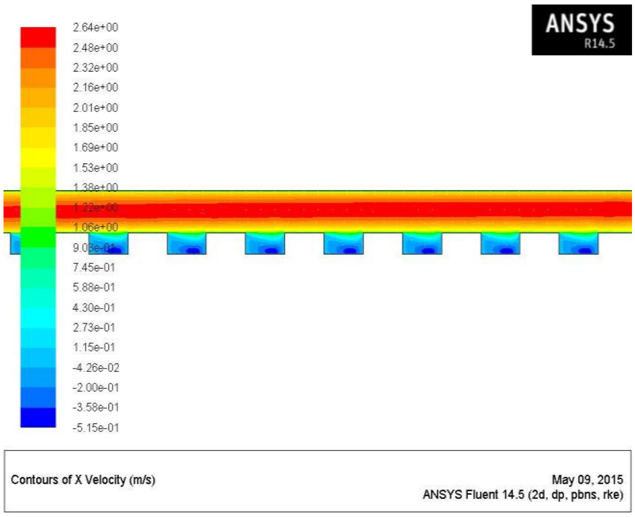

C

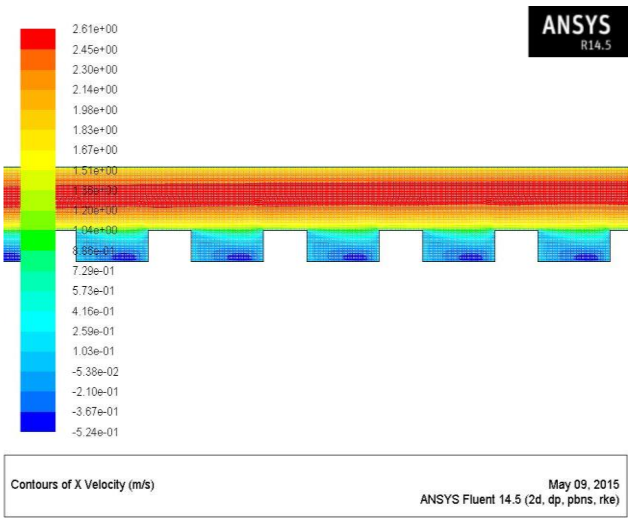

D

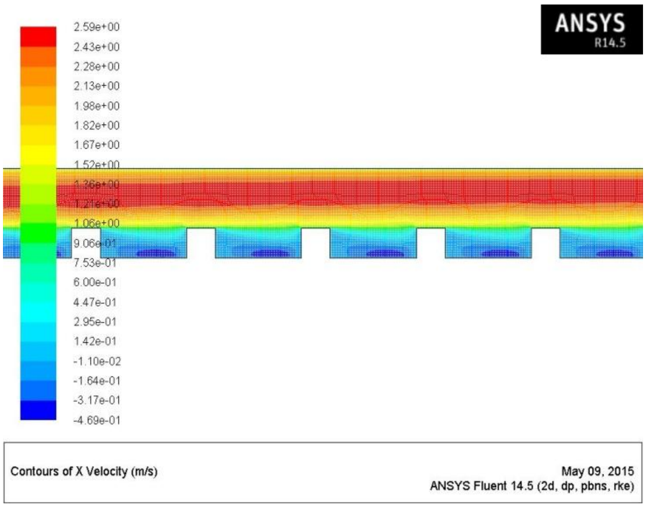

E

Figure 5: Contours of X-velocity (A=0.5,B=0.75,C=1,D=1.25,E=1.5)

7. Conclusions

Numerical investigation of forced convection in a two-dimensional turbulent channel with periodic transverse grooves on the lower channelfor examining heat transfer and friction factor is performed. Validation of the heat transfer for grooved channel is performed by comparing with previous research. Comparison with earlier research shows that Realizable k-ε turbulent model also provide similar results. Increment in heat transfer for B/H= 0.75 is 167% to 199%.

References

[1] Lorenz, S., Mukomilow, D., Leiner, W., "Distribution of the heat transfer coefficient in a channel with periodic transverse grooves" *Experimental Thermal and Fluid Sciences*, 1995, Vol. 11, pp. 234-242

[2] Jaurker, A.R., Saini, J.S., Gandhi, B.K., "Heat transfer and friction characteristics of rectangular solar air heater duct using rib-grooved artificial roughness" *Solar Energy*, 2006, 80, pp. 895-907.

[3] Eiamsa-ard, S., Promvonge, P., "Numerical study on heat transfer of turbulent channel flow over periodic grooves" *International Communications in Heat and Mass Transfer*, 2008, 35, pp. 844-852.

[4] Sahu, R.K. and Gandhi, B.K., "Numerical simulation of heat transfer enhancement due to a gap in an inclined continuous rib arrangement in a solar air heater duct" *International Journal of Advanced Mechanical Engineering*, 2014, Vol. 4, No. 6, pp. 687-693.

[5] Kim Kwang-Yong & Lee Young-Mo, "Design optimization of internal cooling passage with V-shaped ribs" *Numerical Heat Transfer, Part A: Applications: An International Journal of Computation and Methodology*, 2007, 51:11, pp. 1103-1118.

[6] Luo, D.D., Leung, C.W., Chan, T.L. and Wong, W.O., "Flow and forced-convection characteristics of turbulent flow through parallel plates with periodic transverse ribs" *Numerical Heat Transfer, Part A: Applications: An International Journal of Computation and Methodology*, 2005, 48:1, pp. 43-58.

[7] Chaube, A., Sahoo, P.K., Solanki, S.C., "Analysis of heat transfer augmentation and flow characteristics due to rib roughness over absorber plate of a solar air heater" *Renewable Energy*, 2006, 31, pp. 317-331.